Journal of Solid State Chemistry **145,** 643–648 (1999)
Article ID jssc.1999.8269, available online at http://www.idealibrary.com on IDEAL®

A Vanadium (V) Monophosphate with a Tunnel Structure: $KV_2O_4PO_4$

F. Berrah, M. M. Borel, A. Leclaire, M. Daturi, and B. Raveau

Laboratoire CRISMAT, UMR 6508 associée au CNRS, ISMRA et Université de Caen, 6, Boulevard du Maréchal Juin, 14050 CAEN Cedex, France

Received December 30, 1998; in revised form February 24, 1999; accepted March 10, 1999

A vanadium (V) monophosphate, $KV_2O_4PO_4$, with an original tunnel structure has been synthesized. It crystallizes in the space group $Pn2_1a$, with $a = 13.924(1)$ Å, $b = 19.946(1)$ Å, $c = 4.749(1)$ Å. The $[V_2PO_8]_\infty$ framework consists of 90° oriented $[V_2O_8]_\infty$ pyramidal chains running along a and c, respectively, interconnected by single PO_4 tetrahedra. This framework delimits two sets of tunnels: large S-shaped and smaller eight-sided tunnels running along c and a respectively. The K^+ cations are located approximately at the intersection of these tunnels, with an eight- and nine-fold coordination, respectively. The geometry of the chains of corner-sharing VO_5 pyramids is compared to those of the octahedral chains in the perovskite and hexagonal tungsten bronze structures. The existence of two abnormally short V–O bonds per pyramid is emphasized and discussed.

INTRODUCTION

Vanadium phosphates have been extensively explored due to the great potentiality that they offer for the generation of new catalysts, as shown for instance in the V–P–O system (1–2). The structures of the K–V–P–O system performed these last 10 years have allowed a large number of phosphates of tetravalent vanadium (3–8) and of trivalent vanadium (9–12) with original structure to be isolated.

In contrast, only one pentavalent vanadium phosphate, $K_2VO_2PO_4$, has been isolated to date in the system K–V–P–O (13). Nevertheless, phase diagram studies of the latter system performed by several authors a long time ago (14–18) suggest the existence of several other vanadium (V) phosphates besides $K_2VO_2PO_4$. We have thus revisited the system K_2O–V_2O_5–P_2O_5. We report herein on a new vanadium (V) phosphate, $KV_2O_4PO_4$, with an original tridimensional framework built up of corner-sharing VO_5 pyramids and PO_4 tetrahedra forming tunnels occupied by potassium cations.

EXPERIMENTAL SECTION

Solid State Synthesis

Various compositions corresponding to different ratios $K_2O : V_2O_5 : P_2O_5$ were explored systematically. A new phase was isolated for the molar ratios 1 : 2 : 1. Thus, the vanadium (V) monophosphate $KV_2O_4PO_4$ was synthesized in air in two steps. First an intimate stoichiometric mixture of K_2CO_3 and $H(NH_4)_2PO_4$ was heated at 673 K for 2 hours in a platinum crucible to decompose the potassium carbonate and the diammonium hydrogenophosphate. In a second step, the resulting mixture was added with the required amount of V_2O_5, heated up to 798 K for 12 hours, and quenched to room temperature. In these conditions, a monophasic yellow powdered sample is obtained, whose powder X-ray diffraction pattern can be indexed in an orthorhombic cell, in agreement with the parameters determined from the single crystal X-ray study (Table 1).

Crystal Growth

Attempts to grow single crystals of this new phosphate using solid state reactions with the two steps method described above in air were unsuccessful. Then a second solid state reaction procedure was used in which the first step was identical to that described above, whereas the second step was performed in a silica ampoule, heating the mixture up to 823 K for 48 hours and then quenching to room temperature. With this method, yellow plate-like crystals were obtained. The EDS analysis of these crystals confirmed the expected K : V : P composition equal to 1 : 2 : 1. But the poor quality of those crystals and their too small size did not allow their structure determination.

In order to grow larger crystals with a better quality, hydrothermal conditions were used. A mixture of 0.545 g V_2O_5 (99.9 Aldrich) and 0.207 g K_2CO_3 (99.5 Prolabo), finely ground, was introduced in a 23 ml teflon container with 0.342 g H_3PO_4 (75% Prolabo) and 3 ml distilled H_2O. The teflon container placed in a steel autoclave was heated at 493 K for 20 hours and then slowly cooled to room temperature (2.5 K h^{-1}). Well faceted yellow crystals were identified as the $KV_2O_4PO_4$ monophosphate, mixed with an unidentified black yellow powder. Those high quality crystals were used for structure determination.

0022-4596/99 $30.00

TABLE 1
Summary of Crystal Data, Intensity Measurements, and Structure Refinement Parameters for $K(VO_2)_2PO_4$

Crystal data	
Space group	$Pn2_1a$
Cell dimensions	$a = 13.9244(6)$ Å
	$b = 19.9459(7)$ Å
	$c = 4.7487(5)$ Å
Volume	1318.9(2) Å^3
Z	4
ρ_{calc} (g.cm^{-3})	2.36
Intensity measurements	
λ(CuKa)	1.5418 Å
Scan mode	ω–θ
Scan width (°)	$1.3 + 0.14 \tan\theta$
Slit aperture (mm)	$1.2 + 0.25 \tan\theta$
Max θ (°)	75
Standard reflections	3 measured every 3600 s
Measured reflections	1392
Reflections with $I > 3\sigma$	1006
Structure solution and refinement	
Parameters refined	127
Agreement factors	$R = 0.040$, $R_W = 0.044$
Weighting scheme	$w = 1/\sigma^2$
Δ/σ max	< 0.01

Structure Determination

A crystal of $K(VO_2)_2PO_4$ with dimensions $0.107 \times 0.055 \times 0.013$ mm^3 was selected for the structure determination. The intensities recorded showed a Laue symmetry *mmm*. The cell parameters initially measured on Weissenberg films and later refined by diffractometric techniques at 293 K with a least-squares refinement based on 25 reflections are listed in Table 1. The systematic absences $k + l = 2n + 1$ for $0kl$ and $h = 2n + 1$ for $hk0$ are consistent with the space groups $Pnma$ and $Pn2_1a$ (other setting $Pna2_1$). The data were collected on a CAD-4 Enraf-Nonius diffractometer with the parameters reported in Table 1. The reflections were corrected for Lorentz and polarization effects, for absorption (Gaussian method), and for secondary extinction. The deconvolution of the Patterson function was consistent only in the noncentrosymmetric space group $Pn2_1a$ and the refinement of the atomic parameters was successful with this latter space group. The atomic coordinates and the anisotropic thermal factors of V and K and the isotropic thermal factors of the other atoms were refined with a full matrix least-squares method which led to $R = 0.040$ and $R_W = 0.044$ and to the atomic parameters reported in Table 2. The thermal factors of the oxygen atoms are spread over a large range (0.6(3) to 2.5(6) Å^2), but Student's f test shows that the B values are equivalent within the error range.

Infrared Study

An FT-IR experiment has been performed on a KBr pressed disk containing 2% of the analyzed phase accurately dispersed and with a KBr beam splitter. The spectra have been recorded by a Nicolet Magna 550 FT-IR spectrometer (resolution 4 cm^{-1}) and treated with the help of the Nicolet OMNIC™ software.

Description of the structure

The projections of the structure of this new V(V) monophosphate along **c** (Fig. 1) and along **a** (Fig. 2) show that the tridimensional $[V_2PO_8]_\infty$ framework consists of corner-sharing VO_5 pyramids and PO_4 tetrahedra forming large S-shaped tunnels running along **c** (Fig. 1) and smaller eight-sided running along **a** (Fig. 2).

In fact this framework can be described by the assemblage of two kinds of pyramidal chains $[V_2O_8]_\infty$ oriented at 90° and interconnected through single PO_4 tetrahedra. The first kind of $[V_2O_8]_\infty$ chains run along **a** (Fig. 1). In those chains, two successive VO_5 pyramids (V_3, V_4) form $\widehat{O\text{–}O\text{–}O}$ angles

TABLE 2
Positional Parameters and Their Estimated Standard Deviations in $K(VO_2)_2PO_4$

Atom	x	y	z	B (Å^2)
V(1)	0.2885(3)	0.35530	0.2043(7)	0.77(6)[a]
V(2)	0.4568(3)	0.3979(1)	0.7039(7)	1.03(7)[a]
V(3)	0.1265(2)	0.1192(3)	0.6542(7)	1.09(7)[a]
V(4)	0.3763(2)	0.1348(3)	0.8339(7)	1.10(7)[a]
P(1)	0.2329(3)	0.2603(3)	0.683(1)	0.84(6)
P(2)	0.0168(3)	0.4970(3)	0.304(1)	0.81(6)
K(1)	0.2894(5)	0.0036(5)	0.2889(9)	2.21(8)[a]
K(2)	0.0307(5)	0.2506(4)	0.197(1)	1.97(8)[a]
O(1)	0.2315(8)	0.4202(6)	0.326(3)	1.3(2)
O(2)	0.3885(8)	0.3508(6)	0.400(2)	1.3(2)
O(3)	0.2269(8)	0.2818(7)	0.378(2)	1.5(2)
O(4)	0.2265(8)	0.3231(6)	−0.125(2)	1.2(2)
O(5)	0.3566(8)	0.4107(6)	−0.103(2)	1.3(2)
O(6)	0.5143(9)	0.3382(7)	0.828(3)	1.7(2)
O(7)	0.5239(8)	0.4366(6)	0.379(2)	1.1(2)
O(8)	0.5220(8)	0.4766(6)	0.881(2)	1.1(2)
O(9)	0.1203(9)	0.1208(9)	0.315(3)	2.0(2)
O(10)	0.244(1)	0.1047(9)	0.736(2)	0.6(3)
O(11)	0.079(1)	0.0304(9)	0.760(2)	1.0(3)
O(12)	0.147(2)	0.216(1)	0.746(2)	0.7(3)
O(13)	0.490(2)	0.152(1)	0.742(2)	2.5(6)
O(14)	0.3764(9)	0.1367(9)	1.174(3)	2.1(2)
O(15)	0.394(2)	0.044(1)	0.754(2)	1.3(4)
O(16)	0.326(1)	0.2188(9)	0.742(2)	1.1(3)

[a] Atoms have been refined anisotropically. Anisotropically refined atoms are given in the form of the isotropic equivalent displacement parameter defined as: $B = \frac{4}{3} \sum_i \sum_j \mathbf{a}_i . \mathbf{b}_j . \beta_{ij}$.

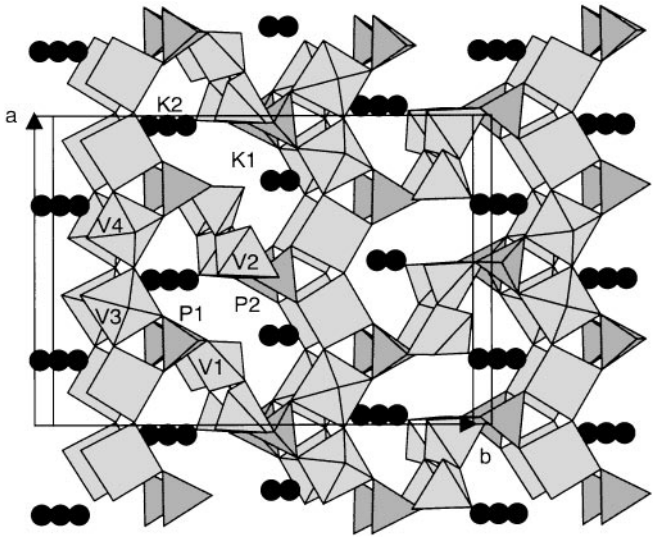

FIG. 1. Projection along **c** of the $KV_2O_4PO_4$ structure showing the large shaped tunnels. The projection axis was tilted 10° to avoid the Esher perspective of edge sharing pyramids on the corner-sharing chains running along **c**.

close to 60° (Fig. 3a), i.e., exhibit a geometry similar to that observed for the chains of WO_6 octahedra in the hexagonal tungsten bronzes (Fig. 3b). Moreover two successive pairs of pyramids have their apical oxygen in a *trans*-position leading to the sequence "*cis-cis-trans-trans*." Note that a similar geometry of $[V_2O_8]_\infty$ pyramidal chains has previously been observed in the ammonium hydrogenophosphate α-$NH_4VO_2PO_3OH$ [19]; however in the latter case the apical oxygens of the pyramids are all in *cis*-position (Fig. 3c). The second kind of $[V_2O_8]_\infty$ chains run along **c** (Fig. 2). In those chains two successive VO_5 pyramids (V_1, V_2) form $\widehat{O\text{–}O\text{–}O}$ angles close to 90° (Fig. 4a) like MO_6 octahedra in the perovskite structure (Fig. 4b). Moreover, two adjacent corner-sharing pyramids have their apical oxygens in a *trans*-position, so that each $[V_2O_8]_\infty$ chain can also be described as built up from two rows of VO_5 pyramids whose apical oxygens are in a *trans*-position with respect to each other (Fig. 4a). The $[V_2O_8]_\infty$ chains are displayed in the form of layers parallel to (0 1 0). Thus, along **b**, one layer of "V_3, V_4" chains alternates with one layer of 'V_1, V_2' chains (Figs. 1, 2), the chains inside each layer being completely isolated. Two successive layers are connected through single PO_4 tetrahedra: each PO_4 tetrahedron shares indeed two apices with one 'V_1, V_2' chain running along **c** and two apices with the next 90° oriented 'V_3, V_4' chain running along **a**.

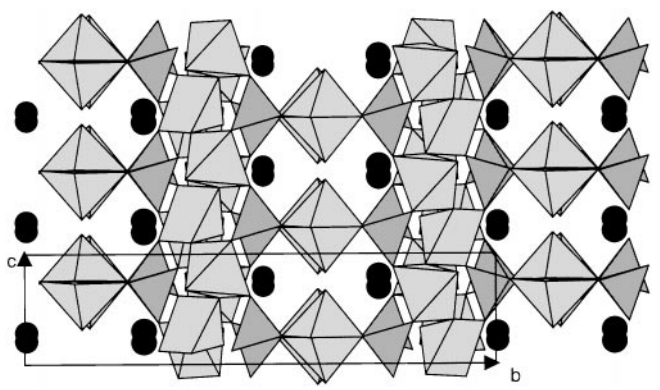

FIG. 2. Projection along **a** of the $KV_2O_4PO_4$ structure showing the height-sided tunnels.

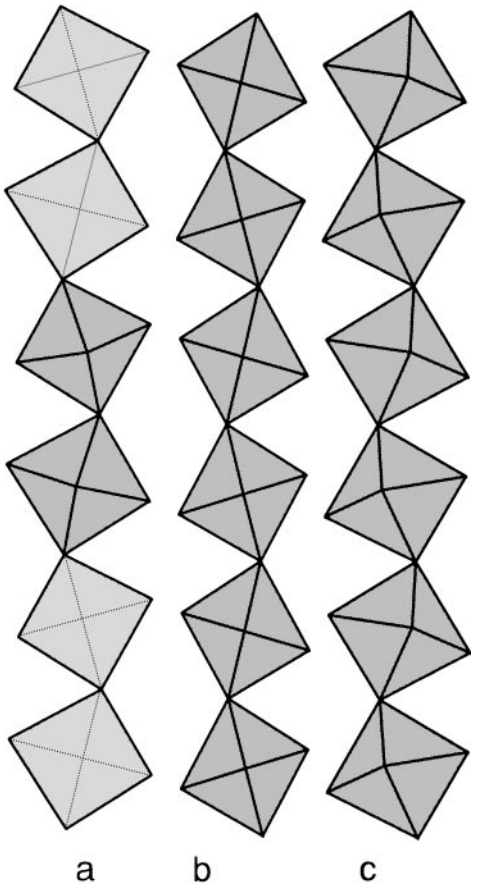

FIG. 3. (a) The $[V_2O_8]_\infty$ chains of corner sharing pyramids running along **a**. (b) The $[WO_5]_\infty$ chains of corner sharing WO_6 octahedra in the hexagonal tungsten bronze. (c) The $[V_2O_8]_\infty$ chains of corner-sharing pyramids in α-$NH_4VO_2PO_3OH$ with all the apical oxygens in *cis*-position.

The geometry of the PO_4 tetrahedra is similar to that usually observed in various monophosphates with P–O bonds ranging from 1.49 to 1.57 Å (Table 3). Similarly, each VO_5 pyramid exhibits a shorter apical V–O bond, ranging from 1.55 to 1.69 Å (Table 3) corresponding to the free apex. In contrast, the nature of the equatorial V–O bonds is rather unexpected. The V_3 and V_4 pyramids exhibit indeed one

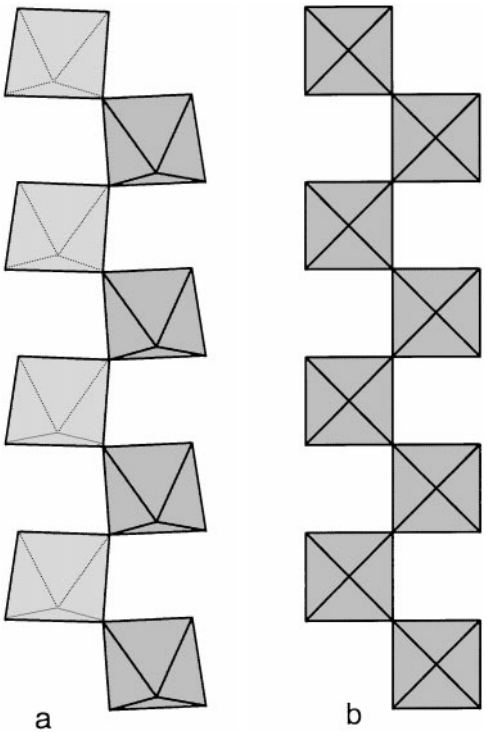

FIG. 4. (a) The $[V_2O_8]_\infty$ chains of corner-sharing pyramids running along **c**. (b) Chain of octahedra in the perovskite structure.

shorter V–O bond (1.68 to 1.70 Å) opposed to a longer one (2.00 to 2.06 Å), corresponding to the $[VO]_\infty$ chain (Fig. 3a), whereas the V–O distances corresponding to the V–O–P bonds are intermediate, ranging from 1.87 to 2.01 Å (Table 3). For the V_1 and V_2 pyramids, one still observes a second abnormally short equatorial V–O distance of 1.68–1.69 Å (Table 3), opposed to a longer one (1.97 to 2.06 Å), corresponding again to a V–O–V bond (Fig. 3b). However in this case, the $[VO]_\infty$ chains are no longer straight, but form 90° oriented V–O–V bonds (Fig. 4a) so that the other equatorial V–O distances corresponding to V–O–P bonds remain close to the longer ones ranging from 1.89 to 2.00 Å (Table 3). Such pyramids involving two abnormally short V–O bonds have already been observed for the phosphate α-$NH_4VO_2PO_3OH$ (19), which exhibits pyramidal chains similar to the first kind of chains encountered here. A similar geometry is also observed for $K_2VO_2PO_4$ (13), but in that case the existence of two abnormally short V–O bonds per pyramid can be explained by the fact that the two corresponding oxygen apices are free. In fact, the great ability of V(V) to be off-centre in the VO_5 pyramids, and especially the alternation of abnormally short and long V–O bonds, seems to be a characteristic of frameworks or chains where VO_5 pyramids share their apices. V_2O_5 itself shows, indeed, besides the vanadyl bond (1.577 Å), rather short V–O bonds (1.779 Å) opposed to long ones (2.017 Å) (20). Bond valence sum calculations using the Brese and O'Keeffe formulations (21) confirm the pentavalent character of vanadium in this new phosphate and agree with the expected valences of the other atoms.

The K^+ cations which are practically located at the intersection of the S-shaped and eight-sided tunnels (Figs. 1,

TABLE 3
Distances (Å) and Angles (°) in the Polyhedra in $K(VO_2)_2PO_4$

V(1)	O(1)	O(2)	O(3)	O(4)	O(5)
O(1)	**1.63(1)**	2.61(2)	2.77(2)	2.89(2)	2.69(2)
O(2)	104.3(6)	**1.68(1)**	2.64(2)	3.41(2)	2.71(1)
O(3)	103.8(6)	95.2(5)	**1.89(1)**	2.53(2)	3.89(2)
O(4)	110.0(6)	144.9(5)	83.8(5)	**1.90(1)**	2.52(2)
O(5)	92.9(5)	92.4(5)	159.3(5)	79.0(5)	**2.06(1)**
V(2)	O(2)	O(6)	O(7)	O(8)	O(5^{i})
O(2)	**1.97(1)**	2.69(2)	2.55(2)	3.87(2)	2.68(1)
O(6)	99.2(6)	**1.55(1)**	2.91(2)	2.77(2)	2.65(2)
O(7)	80.9(5)	110.8(6)	**1.96(1)**	2.51(1)	3.43(1)
O(8)	154.6(5)	102.1(6)	78.8(5)	**2.00(1)**	2.65(2)
O(5^{i})	94.0(5)	103.7(6)	139.5(5)	91.6(5)	**1.69(1)**
V(3)	O(9)	O(10)	O(11)	O(12)	O(13^{ii})
O(9)	**1.62(1)**	2.66(2)	2.84(2)	2.82(2)	2.84(2)
O(10)	106.3(6)	**1.70(2)**	2.73(3)	2.61(3)	3.65(4)
O(11)	104.8(7)	96.4(8)	**1.95(2)**	3.83(3)	2.72(3)
O(12)	101.9(7)	88.8(9)	150.1(5)	**2.01(2)**	2.53(4)
O(13^{ii})	100.6(6)	151.7(6)	85.1(9)	77(1)	**2.06(3)**
V(4)	O(10)	O(13)	O(14)	O(15)	O(16)
O(10)	**2.00(2)**	3.56(3)	2.85(2)	2.42(3)	2.55(3)
O(13)	150.9(6)	**1.68(3)**	2.61(2)	2.54(4)	2.65(3)
O(14)	104.0(6)	104.4(6)	**1.61(2)**	2.73(2)	2.72(2)
O(15)	77.4(9)	91(1)	103.0(7)	**1.87(2)**	3.62(3)
O(16)	82.4(7)	96(1)	102.0(7)	150.7(6)	**1.87(2)**
P(1)	O(3)	O(12)	O(16)	O(4^{i})	
O(3)	**1.51(1)**	2.45(2)	2.54(2)	2.50(2)	
O(12)	108.0(7)	**1.52(2)**	2.49(3)	2.48(3)	
O(16)	111.5(6)	108(1)	**1.56(2)**	2.58(2)	
O(4^{i})	109.2(8)	107.7(8)	111.8(7)	**1.55(1)**	
P(2)	O(15^{iii})	O(11^{iv})	O(7^{v})	O(8^{ii})	
O(15^{iii})	**1.57(2)**	2.59(3)	2.50(3)	2.48(2)	
O(11^{iv})	114(1)	**1.52(2)**	2.42(2)	2.52(2)	
O(7^{v})	109.7(9)	107.3(7)	**1.49(1)**	2.50(1)	
O(8^{ii})	105.3(6)	110.3(6)	110.3(7)	**1.55(1)**	

K(1) – O(15): 2.76(2)	K(2) – O(12^{ix}): 2.77(2)
K(1) – O(1^{vi}): 2.77(1)	K(2) – O(2^{v}): 2.85(1)
K(1) – O(5^{vii}): 2.80(1)	K(2) – O(6^{ii}): 2.86(1)
K(1) – O(8^{viii}): 2.80(2)	K(2) – O(13^{v}): 2.92(2)
K(1) – O(14^{ix}): 2.97(2)	K(2) – O(3): 2.93(1)
K(1) – O(10): 3.00(2)	K(2) – O(9): 2.93(2)
K(1) – O(15^{ix}): 3.03(2)	K(2) – O(6^{v}): 3.05(1)
K(1) – O(1^{vii}): 3.06(1)	K(2) – O(12): 3.14(1)
	K(2) – O(14^{ii}): 3.18(2)

Note. Symmetry codes: (i) x; y; $z+1$. (ii) $+x-1/2$; y; $-z+3/2$. (iii) $-x+1/2$; $y+1/2$; $+z-1/2$. (iv) $-x$; $y+1/2$; $z+1$. (v) $+x-1/2$; y; $-z+1/2$. (vi) $-x+1/2$; $+y-1/2$; $+z-1/2$. (vii) $-x+1/2$; $+y-1/2$; $z+1/2$. (viii) $-x+1$; $+y-1/2$; $-z+1$. (ix) x; y; $+z-1$.

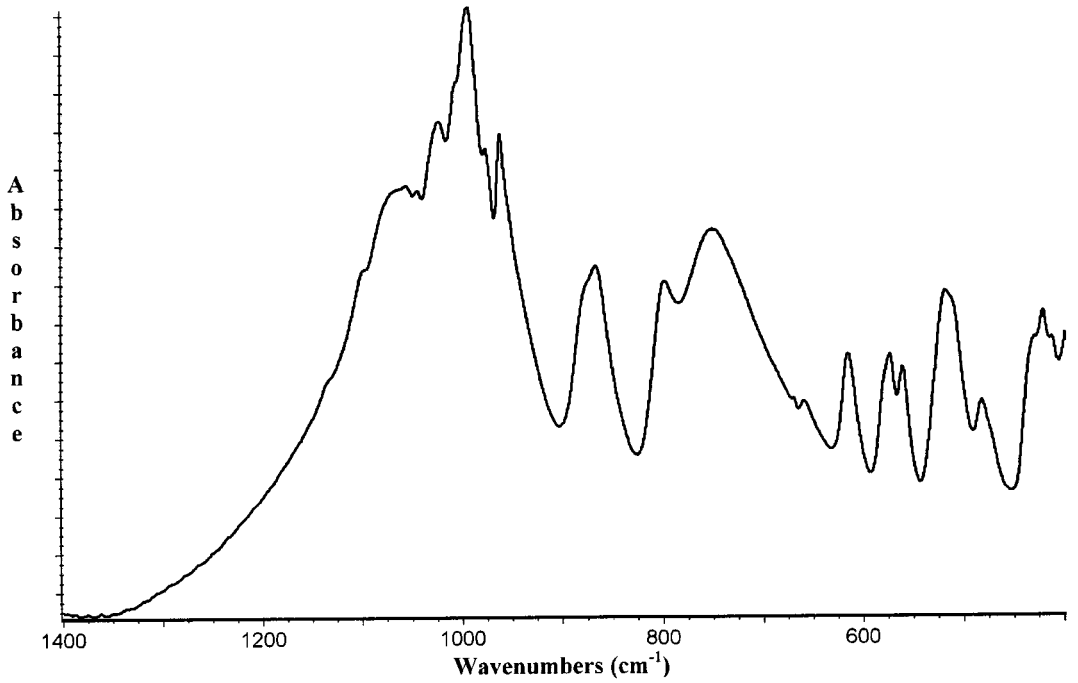

FIG. 5. FT-IR spectrum of $KV_2O_4PO_4$ sample in the skeletal vibration modes region.

2) exhibit two sorts of coordinations. K(1) is surrounded by eight oxygen atoms with distances ranging from 2.76 to 3.06 Å and K(2) is linked to nine oxygen atoms with distances ranging from 2.77 to 3.18 Å.

The infrared spectrum of $KV_2O_4PO_4$ is repeated in Fig. 5. According to the band assignment for parent compounds proposed in the literature (13), ν_{as}P–O and ν_sP–O stretches give rise to the complex mass if in the spectral region 1400–800 cm^{-1}, with the asymmetric modes placed in the higher energy side of that range. Superimposed to those bands we should find the V=O stretches of the free apex of the VO_5 pyramid, likely near the maximum at 994 cm^{-1}. The asymmetric bending δ_{as}O–P–O of the corner-sharing phosphate tetrahedra is responsible for the features between 700 and 600 cm^{-1}, while the corresponding symmetric bending δ_sO–P–O is placed below 450 cm^{-1}. The complexity of the infrared spectrum, the high number of structure components, and the calculations connected with so many atoms in the elemental cell yield a difficult task further distinct in band assignments, such as separation of the modes belonging to different vanadyl chains or isolated VO_5 pyramids.

CONCLUDING REMARKS

This study has allowed a second V(V) phosphate to be synthesized. The existence of large tunnels where K^+ cations are inserted suggests that isotypic phases involving ammonium or methylammonium cations should exist. A systematic study of such phases using hydrothermal synthesis is in progress. In a more general manner, the combination of the two types of $[V_2O_8]_\infty$ pyramidal chains described herein for this structure should lead to the generation of other original frameworks.

REFERENCES

1. G. Centi, F. Trifiro, J. R. Ebner, and V. M. Franchetti, *Chem. Rev.* **88,** 55 (1988).
2. B. L. Hodnett, *Catal. Rev. Sci. Eng.* **27,** 373 (1985).
3. L. Benhamada, A. Grandin, M. M. Borel, A. Leclaire, and B. Raveau, *Acta Cryst. C* **47,** 1138 (1991).
4. K. H. Lii and H. J. Tsai, *J. Solid State Chem.* **87,** 396 (1990).
5. A. Leclaire, H. Chahboun, D. Groult, and B. Raveau, *J. Solid State Chem.* **77,** 170 (1988).
6. Y. E. Gorbunova, S. A. Linde, A. V. Lavrov, and I. V. Tananaev, *Dokl. Akad. Nauk SSSR* **250,** 350 (1980).
7. M. M. Borel, A. Leclaire, J. Chardon, J. Provost, H. Rebbah, and B. Raveau, *J. Solid State Chem.* **132,** 41 (1997).
8. F. Berrah, A. Guesdon, A. Leclaire, M. M. Borel, J. Provost, and B. Raveau, *Acta Cryst.*, in press.
9. L. Benhamada, A. Grandin, M. M. Borel, A. Leclaire, and B. Raveau, *Acta Cryst. C* **47,** 424 (1991).
10. L. Benhamada, A. Grandin, M. M. Borel, A. Leclaire, and B. Raveau, *J. Solid State Chem.* **91,** 264 (1991).
11. L. Benhamada, A. Grandin, M. M. Borel, A. Leclaire, and B. Raveau, *J. Solid State Chem.* **104,** 193 (1993).

12. A. Benmoussa, M. M. Borel, A. Grandin, A. Leclaire, and B. Raveau, *J. Solid State Chem.* **97,** 314 (1992).
13. V. C. Korthuis, R. D. Hoffmann, J. Huang, and A. W. Sleight, *Chem. Mat.* **5,** 206 (1993).
14. V. V. Illarionov, R. P. Ozerov, and E. V. Kil'Disheva, *Russ. J. Inorg. Chem.* **5,** 1352 (1960).
15. A. G. Bergman and Z. I. Sanzharova, *Russ. J. Inorg. Chem.* **15,** 581 (1970).
16. A. G. Bergman and Z. I. Sanzharova, *Russ. J. Inorg. Chem.* **15,** 877 (1970).
17. F. Preuss and H. Sching, *Z. Naturforsh* **30b,** 334 (1975).
18. V. V. Illarionov, A. L. Soklakov, and E. V. Kil'Disheva, *Russ. J. Inorg. Chem.* **6,** 691 (1961).
19. P. Amoros and A. Lebail, *J. Solid State Chem.* **97,** 283 (1992).
20. A. Bystrom, K. A. Wilhelmi, and O. Brotzen, *Acta Chem. Scand.* **4,** 1119 (1950).
21. N. E. Brese and M. O'Keeffe, *Acta Cryst. B* **47,** 192 (1991).